

Numerical Simulation of Moisture Diffusion in Pultruded GFRP Composite Profile

Haohui Xin^{1,2}^a, Ayman Mosallam³^b, Yuqing Liu^{2,*}^c

¹*School of Human Settlements and Civil Engineering, Xi'an Jiaotong University, Xi'an, China;*

²*Department of Bridge Engineering, Tongji University, Shanghai, China*

³*Department of Civil and Environment Engineering, University of California, Irvine, CA, USA*

Keywords: Pultruded fiber-reinforced polymer (FRP) materials; Non-Fick Moisture Diffusion; Numerical Simulation.

Abstract: Long-term exposure of fiber-reinforced polymer (FRP) profile to harsh in-service environment will lead to irreversible degradation of mechanical properties. Understanding the exposure “aging” effects on pultruded FRP composites is important for their application in bridge structures. The moisture diffusion process plays a very important role to understand material degradation of GFRP laminations exposed to hydrothermal environment. In this paper, the moisture diffusion process with focusing on pultruded GFRP composites used in bridge applications is numerically simulated. The parameters of moisture diffusion are calibrated by gravimetric tests of thin plates.


1 INTRODUCTION


Pultruded glass fiber-reinforced polymer (GFRP) is favorable by civil engineers because its economic elegant performance (Bank, 2006; Mosallam, Bayraktar, Elmikawi, Pul, & Adanur, 2014). Several GFRP profiles have been exploited in bridge structures (Bank, 2006; Mosallam et al., 2014; Xin, Liu, & Du, 2015; Xin, Liu, He, Fan, & Zhang, 2015; Xin, Liu, Mosallam, He, & Du, 2017; Xin et al., 2020; Xin, Mosallam, Liu, Veljkovic, & He, 2019; Xin, Mosallam, Liu, Wang, & Zhang, 2017a; Xin, Mosallam, Liu, Wang, & He, 2018; Xin, Mosallam, Liu, Xiao, et al., 2017; Xiong, Liu, Zuo, & Xin, 2019; Zhang et al., 2019; Zuo, Mosallam, Xin, Liu, & He, 2018). Bridge structures are generally exposed to harsh in-service environment. The temperature and humidity varied a lot (Xin, Liu, Mosallam, & Zhang, 2016; Xin, Liu, Mosallam, Zhang, & Wang, 2016; Xin, Mosallam, Liu, & Wang, 2018; Xin, Mosallam, Liu, Wang, & Zhang, 2017b; Xin, Mosallam, Liu, Yang, & Zhang, 2017). Long-term exposure of fiber-reinforced polymer (FRP) profile to harsh in-service environment will lead to irreversible degradation of mechanical properties. The performance degradation


due to aging may lead to catastrophic failure of bridge structural component. While the moisture diffusion process plays a very important role to understand material degradation of GFRP laminations exposed to hydrothermal environment.

Hence, it is essential to understand the moisture diffusion process with focusing on pultruded GFRP composites used in bridge applications. The authors' previous publication (Xin, Liu, Mosallam, & Zhang, 2016) showed that the moisture uptakes of pultruded GFRP plate could be divided into three stages: diffusion-dominated uptake, a polymer relaxation-dominated uptake and a composite damage-dominated uptake. The non-Fick moisture diffusion is quite important to understand material degradation of GFRP laminations exposed to hydrothermal environment. Investigation of non-Fick moisture diffusion process with time will benefit to reveal the aging degradation mechanism of GFRP profiles serviced as components of bridge structures. Numerical simulation is an efficient tool to model the moisture diffusion of bridge profile with complicated geometry.

The moisture progression with focusing on pultruded GFRP profiles serviced as components of bridge structures is numerically simulated in this

^a <https://orcid.org/0000-0002-6205-5248>

^b <https://orcid.org/0000-0002-1897-1775>

^c <https://orcid.org/0000-0002-1211-0018>

paper. The parameters of moisture diffusion are calibrated by gravimetric tests of thin plates (100.0mm×6.0mm×2.3mm) at different temperature and different environment.

2 GRAVIMETRIC TESTS

Pultruded GFRP laminations for the tests are cut form GFRP profiles serviced as a component of bridge structures(ASTM D5229/D5229M-14 Standard, 2014). The laminates include three types of lamina, namely Roving, axial compound fabric and biaxial compound fabric, see Fig. 1. The experiment is conducted in four hygrothermal environment, namely T_W(water) and T_SW(artificial seawater), T=40°C and 60°C, based on the ASTM D5229/D5229M procedures(ASTM D5229/D5229M-14 Standard, 2014). The details of gravimetric experiment can be referred to (Xin, Liu, Mosallam, & Zhang, 2016).

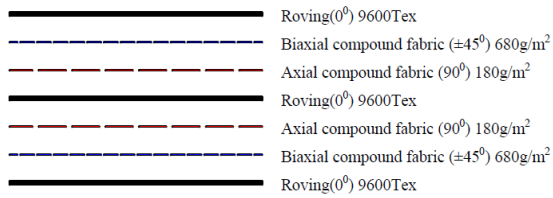


Figure 1: Configurations of GFRP laminate (Xin, Liu, Mosallam, & Zhang, 2016)

The gravimetric tests of thin plates with a dimension of 100.0mm×6.0mm×2.3mm were used for the one dimensional moisture diffusion of pultruded GFRP laminates in the authors' previous publication(Xin, Liu, Mosallam, & Zhang, 2016). D11 denoted the specimens along the roving direction while D22 denoted the specimens vertical to the roving direction. The parameters of time-varying boundary conditions are calibrated by gravimetric tests of this thin plates at different temperature and environment.

3 MASS DIFFUSION SIMULATION OF GFRP LAMINATIONS

Mass diffusion analysis is performed using three-dimensional solid elements DC3D8 with a 1mm mesh size based on commercial finite element software ABAQUS(Abaqus, 2019). Eq. (1) is used to obtain

the mass concentration through a Python script to read the ABAQUS simulation data.

$$C(t) = \frac{\sum_{i=1}^n C_i(t)V_i}{\sum_{i=1}^n V_i} \quad (1)$$

Where: C_i is the mass concentration of the i^{th} integration point, and V_i is the volume of the i^{th} integration point.

The experimental results were given as weight gain $M(t)$ in percentage against time (Xin, Liu, Mosallam, & Zhang, 2016). The average concentration could be converted to the weight-gain data by equations (2).

$$M(t) = \frac{\rho_{water}}{\rho_{GFRP}} C(t) \quad (2)$$

Where: $\rho_{GFRP}=2000 \text{ kg/m}^3$ is the density of the pultruded GFRP laminations, $\rho_{water}=1000\text{kg/m}^3$ is the density of the water.

The moisture diffusion coefficients of pultruded GFRP laminates can be referred to the reference (Xin, Liu, Mosallam, & Zhang, 2016). For the one-dimensional diffusion, the time-varying boundary is applied to the largest cross section, see Fig. 2. Based on the experimental results(Xin, Liu, Mosallam, & Zhang, 2016), the moisture uptake along the roving direction is larger than it vertical to roving direction. The magnitude of mass concentration is assumed to be 1.0. The non-Fick behavior of moisture diffusion is mainly controlled by the amplitude of multi-stage points of amplitude function.

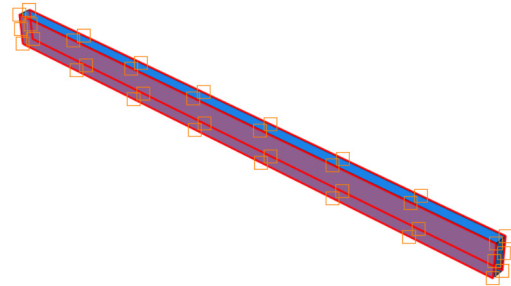


Figure 2: Illustration of time-varying boundary conditions of one-dimensional diffusion

4 EXPOSED TO ENVIRONMENT WITH A TEMPERATURE OF 40°C

The values of multi-stage points of the amplitude function were determined by conducting the fit on the

moisture uptake at the temperature of 40°C. The comparisons between FE simulation and experimental moisture uptake of specimens at the temperature of 40°C are shown in Fig.3 and Fig.4, respectively. A good agreement is observed. The fitted time-varying boundary conditions could effectively describe the one-dimensional moisture migration of GFRP specimens exposed to 40°C hydrothermal environment.

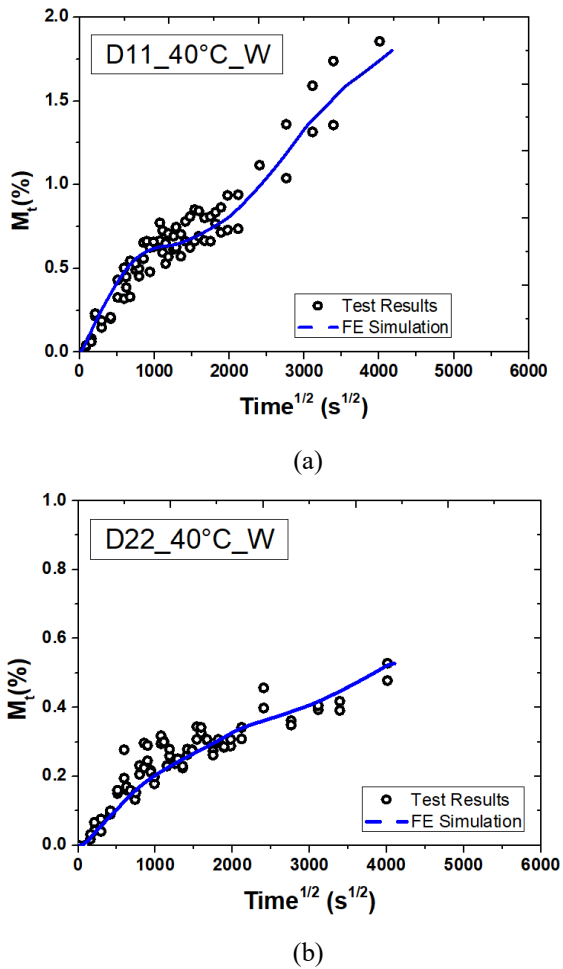


Figure 3: Comparisons between FE simulation and experimental moisture uptake of specimens exposed to water environment at 40°C

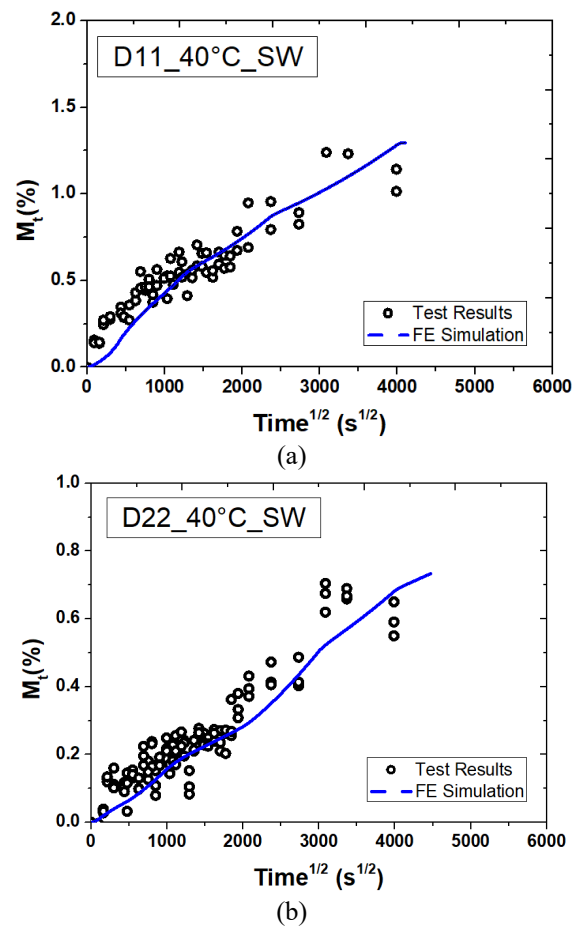
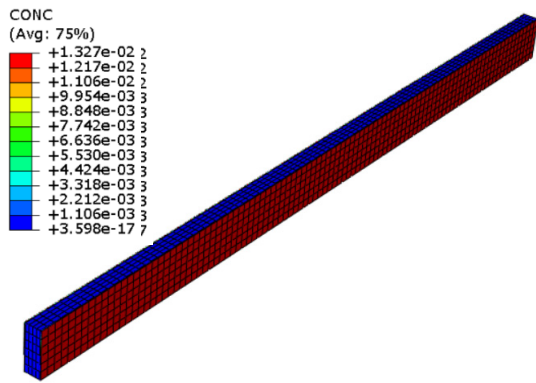
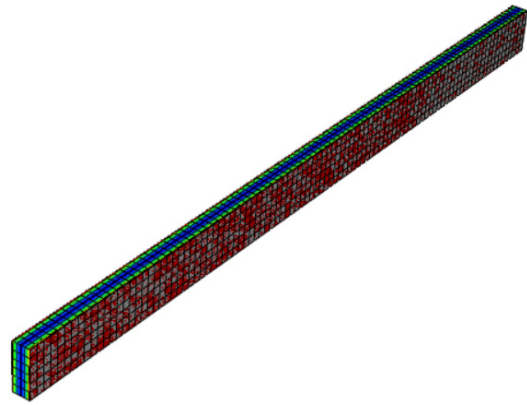


Figure 4: Comparisons between FE simulation and experimental moisture uptake of specimens exposed to artificial seawater environment at 40°C

The moisture diffusion process of D11 and D22 specimens at the temperature of 40°C is shown in Fig.5 and Fig.6. The minimum CONC at the inner side reached to 97.3% and 99.2% times of CONC at the out surface for D11 specimen at 1.70×10^6 s and 1.70×10^7 s respectively, and increased to 88.0% and 99.2% times of CONC at the out surface for D22 specimen at 1.73×10^6 s and 1.70×10^7 s respectively.

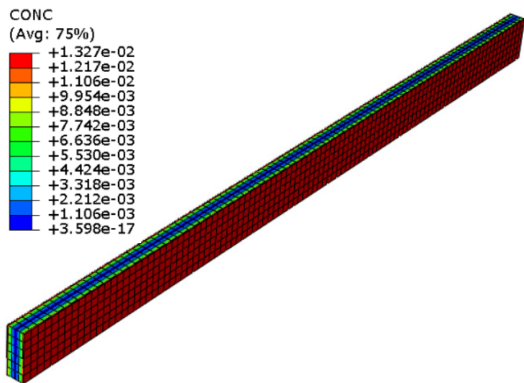


(a) $t = 9.0 \text{ s}$

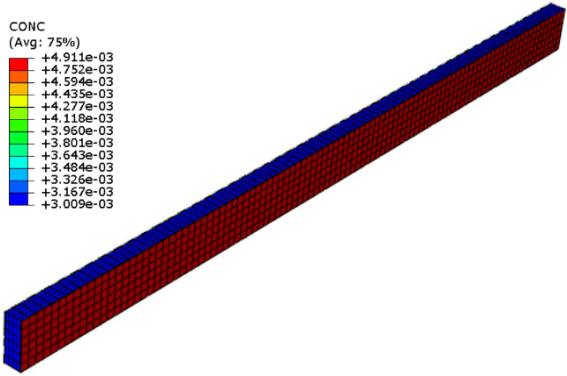


(d) $t = 1.70 \times 10^7 \text{ s}$

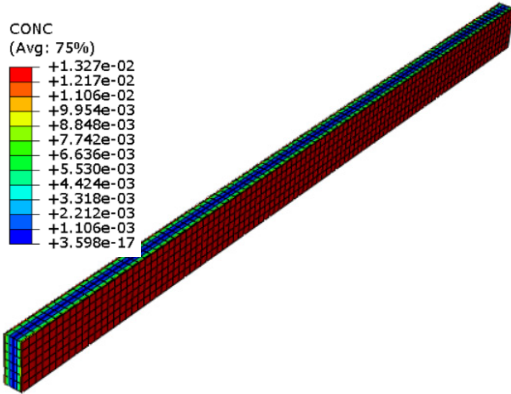
Figure 5: One dimensional diffusion of D11 specimen exposed to water environment at 40°C



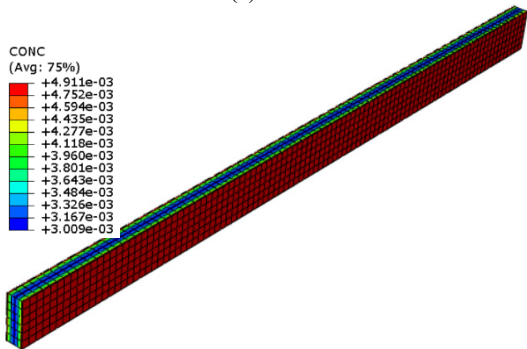
(b) $t = 4.1 \times 10^5 \text{ s}$



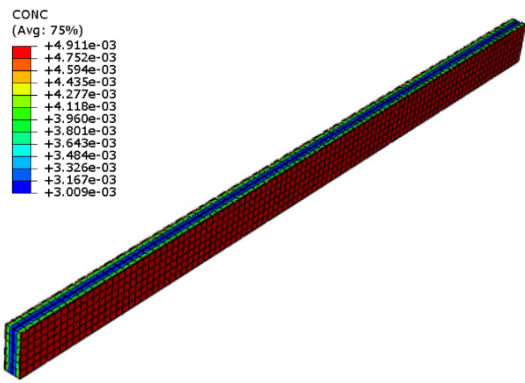
(a) $t = 9.0 \text{ s}$



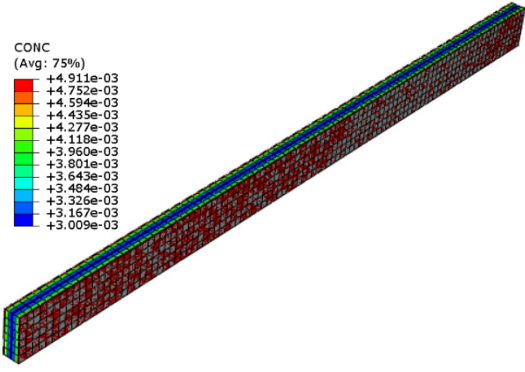
(c) $t = 1.7 \times 10^6 \text{ s}$



(b) $t = 7.31 \times 10^5 \text{ s}$



(c) $t=1.7 \times 10^6$ s

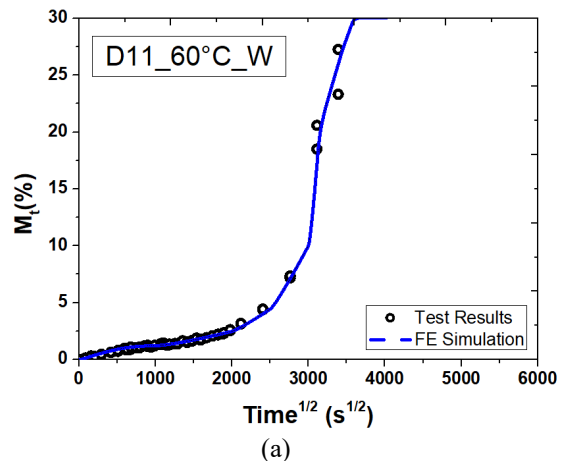


(d) $t=1.7 \times 10^7$ s

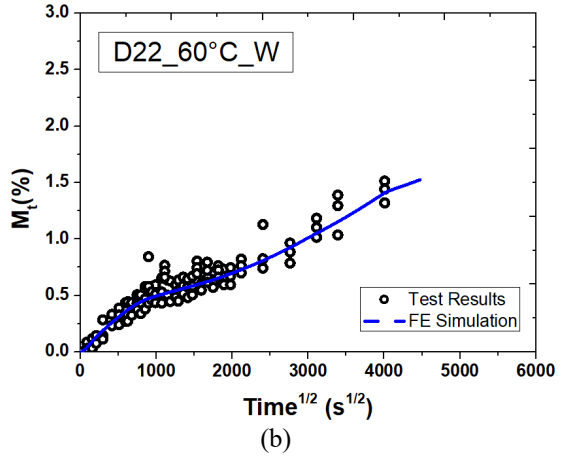
Figure 6: One dimensional diffusion of D22 specimen exposed to water environment at 40°C

5 EXPOSED TO ENVIRONMENT WITH A TEMPERATURE OF 60°C

The values of multi-stage points of the amplitude function were determined by conducting the fit on the moisture uptake at the temperature of 60°C. The comparisons between FE simulation and experimental moisture uptake at 60°C are shown in Fig. 7 and Fig. 8, respectively. A good agreement is observed, indicating that the fitted time-varying boundary conditions could effectively describe the one-dimensional moisture migration of GFRP specimens exposed to 60°C hygrothermal environment.

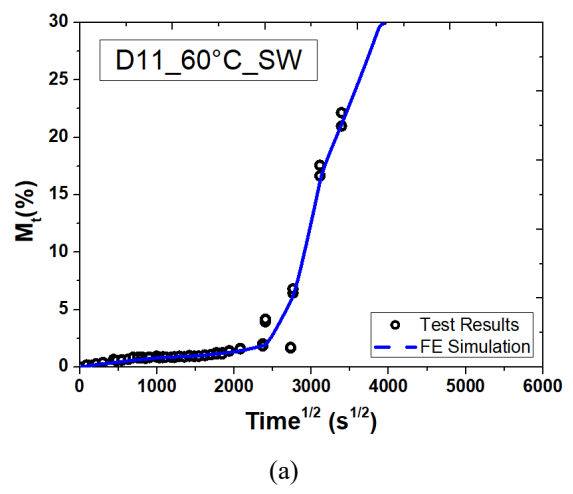


(a)



(b)

Figure 7: Comparisons between FE simulation and experimental moisture uptake of specimens exposed to water environment at 60°C



(a)

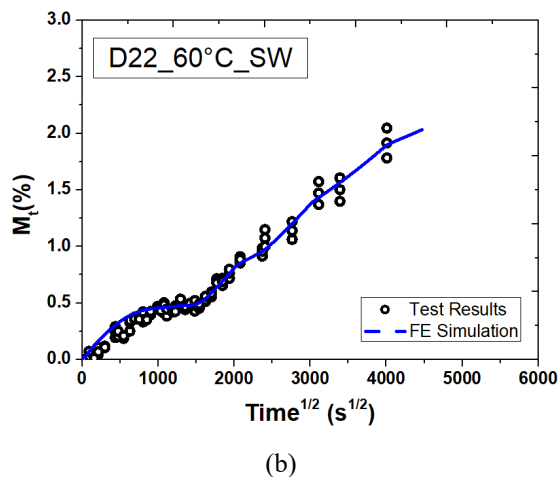
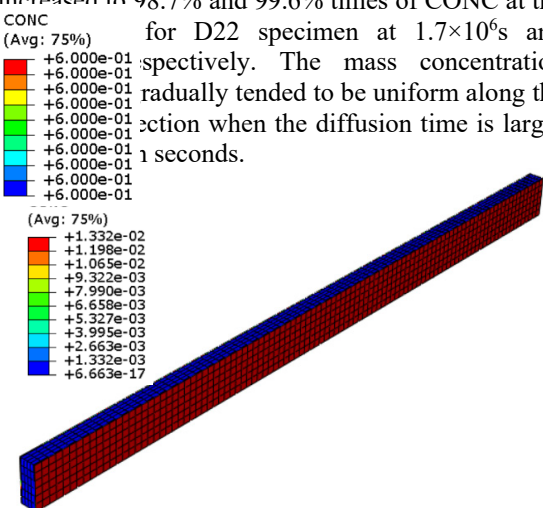
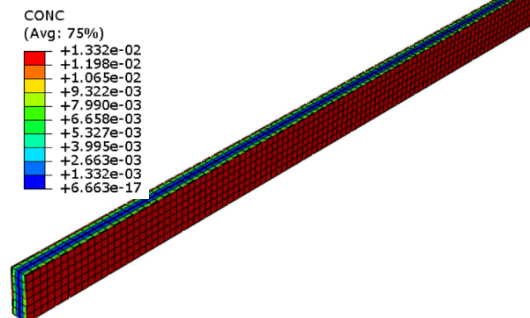


Figure 8. Comparisons between FE simulation and experimental moisture uptake of specimens exposed to artificial seawater environment at 60°C

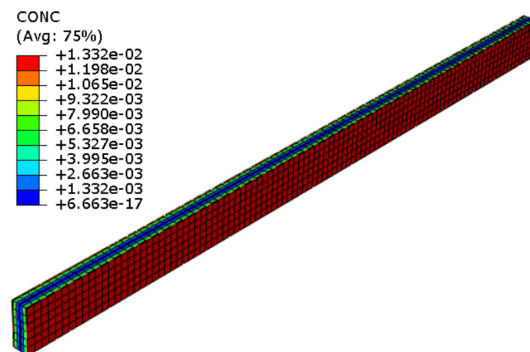
The moisture diffusion process of D11 and D22 specimens exposed to artificial seawater environment is shown in Fig.9 and Fig.10. With the diffusion time increasing, the CONC of inner side gradually increased. The mass concentration presented gradient distribution along the thickness direction. The minimum CONC at the inner side reached 96.3% and 100.0% times of CONC at the out surface for D11 specimen at 1.7×10^6 s and 1.7×10^7 s, respectively, and increased to 98.7% and 99.6% times of CONC at the inner side for D22 specimen at 1.7×10^6 s and 1.7×10^7 s, respectively. The mass concentration gradually tended to be uniform along the thickness direction when the diffusion time is larger than 10000 seconds.



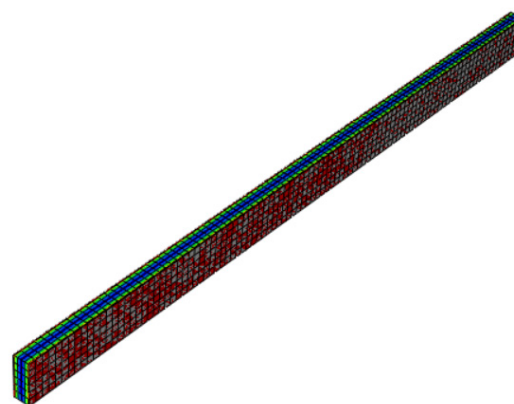
(a) $t=9.0$ s



(b) $t=7.3 \times 10^5$ s

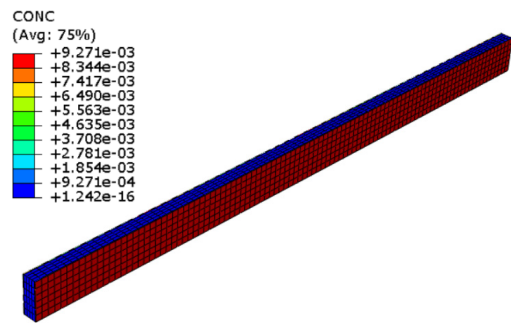


(c) $t=1.7 \times 10^6$ s

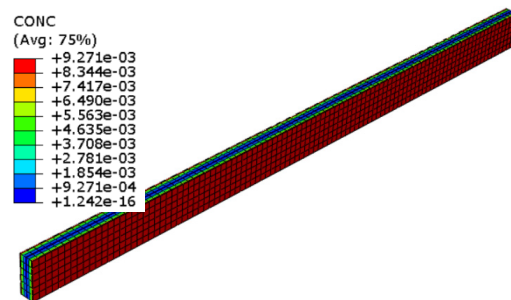


(d) $t=1.7 \times 10^7$ s

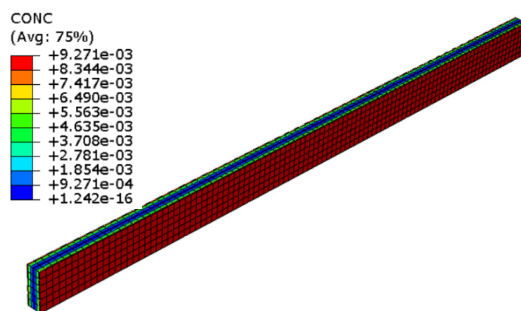
Figure 9. One dimensional diffusion of D11 specimen exposed to artificial seawater environment at 60°C



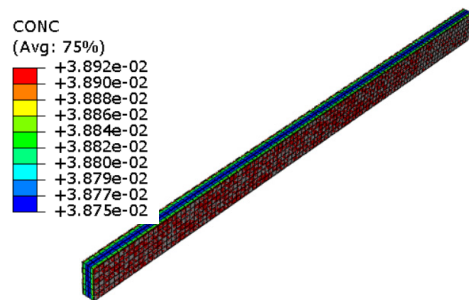
(a) $t=9.0s$



(b) $t=7.3 \times 10^5 s$



(c) $t=1.7 \times 10^6 s$



(d) $t=1.7 \times 10^7 s$

Figure 10. One dimensional diffusion of D22 specimen exposed to artificial seawater environment at 60°C

6 CONCLUSIONS

Long-term exposure of fiber-reinforced polymer (FRP) profile to harsh in-service environment will lead to irreversible degradation of mechanical properties. Understanding the exposure “aging” effects on pultruded FRP composites is important for their application in bridge structures. The moisture diffusion process plays a very important role to understand material degradation of GFRP laminations exposed to hydrothermal environment.

The parameters of moisture diffusion are calibrated by gravimetric tests of thin plates (one-dimensional diffusion). The calibrated mass diffusion parameters are validated by comparing the average time-dependent moisture concentration obtained from non-Fick FE simulation with experimental observation.

For one-dimensional moisture diffusion of thin plates, with the diffusion time increasing, the CONC of inner side gradually increased. With the diffusion time increasing, the CONC of inner side gradually increased. The mass concentration presented gradient distribution along the thickness direction gradually. The mass concentration distribution gradually tended to be uniform along the thickness direction when the diffusion time is larger than 1 million seconds.

ACKNOWLEDGEMENTS

The authors gratefully acknowledge the financial support provided by the National Natural Science Foundation (Grants #51808398 and 52078362) of the People’s Republic of China.

REFERENCES

- Abaqus, V. (2019). 2019 Documentation. *Dassault Systemes Simulia Corporation*, 651.
- ASTM D5229/D5229M-14 Standard. (2014). Standard Test Method for Moisture Absorption Properties and Equilibrium Conditioning of Polymer Matrix Composite Materials. *STM International*, 100 Barr Harbor Drive, PO Box C700, West Conshohocken, PA, 19428-2959 USA.
- Bank, L. C. (2006). Composites for Construction. In *Composites for Construction: Structural Design with FRP* *Materials*. <https://doi.org/10.1002/9780470121429>
- Mosallam, A. S., Bayraktar, A., Elmikawi, M., Pul, S., & Adanur, S. (2014). Polymer Composites in

- Construction: An Overview. *Review Article of SOJ Materials Science & Engineering*.
- Xin, H., Liu, Y., & Du, A. (2015). *Thermal analysis on composite girder with hybrid GFRP-concrete deck*. 5.
- Xin, H., Liu, Y., He, J., Fan, H., & Zhang, Y. (2015). *Fatigue behavior of hybrid GFRP-concrete bridge decks under sagging moment*. 4, 925–946.
- Xin, H., Liu, Y., Mosallam, A. S., He, J., & Du, A. (2017). Evaluation on material behaviors of pultruded glass fiber reinforced polymer (GFRP) laminates. *Composite Structures*, 182, 283–300. <https://doi.org/10.1016/j.compstruct.2017.09.006>
- Xin, H., Liu, Y., Mosallam, A., & Zhang, Y. (2016). Moisture diffusion and hygrothermal aging of pultruded glass fiber reinforced polymer laminates in bridge application. *Composites Part B: Engineering*, 100, 197–207. <https://doi.org/10.1016/j.compositesb.2016.04.085>
- Xin, H., Liu, Y., Mosallam, A., Zhang, Y., & Wang, C. (2016). *Hygrothermal aging effects on flexural behavior of pultruded glass fiber reinforced polymer laminates in bridge applications*. 127, 237–247.
- Xin, H., Mosallam, A., Correia, J. A. F. O., Liu, Y., He, J., & Sun, Y. (2020). Material-structure integrated design optimization of GFRP bridge deck on steel girder. *Structures*, 27, 1222–1230. Elsevier.
- Xin, H., Mosallam, A., Liu, Y., Veljkovic, M., & He, J. (2019). Mechanical characterization of a unidirectional pultruded composite lamina using micromechanics and numerical homogenization. *Construction and Building Materials*, 216, 101–118.
- Xin, H., Mosallam, A., Liu, Y., & Wang, C. (2018). Hygrothermal aging effects on axial behaviour of pultruded web-flange junctions and adhesively bonded build-up bridge members. *Journal of Reinforced Plastics and Composites*, 37(1), 13–34.
- Xin, H., Mosallam, A., Liu, Y., Wang, C., & Zhang, Y. (2017a). *Analytical and experimental evaluation of flexural behavior of FRP pultruded composite profiles for bridge deck structural design*. 150, 123–149.
- Xin, H., Mosallam, A., Liu, Y., Wang, C., & Zhang, Y. (2017b). Impact of hygrothermal aging on rotational behavior of web-flange junctions of structural pultruded composite members for bridge applications. *Composites Part B*, 110, 279–297. <https://doi.org/10.1016/j.compositesb.2016.09.105>
- Xin, H., Mosallam, A., Liu, Y., Xiao, Y., He, J., Wang, C., & Jiang, Z. (2017). Experimental and numerical investigation on in-plane compression and shear performance of a pultruded GFRP composite bridge deck. *Composite Structures*, 180, 914–932. <https://doi.org/10.1016/j.compstruct.2017.08.066>
- Xin, H., Mosallam, A., Liu, Y., Yang, F., & Zhang, Y. (2017). Hygrothermal aging effects on shear behavior of pultruded FRP composite web-flange junctions in bridge application. *Composites Part B: Engineering*, 110, 213–228. <https://doi.org/10.1016/j.compositesb.2016.10.093>
- Xin, H., Mosallam, A. S., Liu, Y., Wang, C., & He, J. (2018). Experimental and numerical investigation on assessing local bearing behavior of a pultruded GFRP bridge deck. *Composite Structures*, 204, 712–730.
- Xiong, Z., Liu, Y., Zuo, Y., & Xin, H. (2019). Experimental evaluation of shear behavior of pultruded GFRP perforated connectors embedded in concrete. *Composite Structures*, 222, 110938.
- Zhang, Y., Mosallam, A., Liu, Y., Sun, Y., Xin, H., & He, J. (2019). Assessment of Flexural Behavior of Pultruded GFRP Laminates for Bridge Deck Applications. *Advances in Materials Science and Engineering*, 2019.
- Zuo, Y., Mosallam, A., Xin, H., Liu, Y., & He, J. (2018). Flexural performance of a hybrid GFRP-concrete bridge deck with composite T-shaped perforated rib connectors. *Composite Structures*, 194, 263–278.